Hysteretic Behavior Of CHS T-Joints With Doubler Reinforcement Under Cyclic Loading

Hanan H. Eltobgy, Emad Darwish, Mohamed A. Aboshok

Abstract: Welded circular hollow section joints subjected to cyclic loads are prone to crack propagation contributing to failure at the welded toe due to the fragile stiffness of the chord joint at its radial direction. The tubular chord connection equipped with a brace can be reinforced by a doubler plate to increase the chord stiffness and avoid such failure. In this research experimental and analytical investigations were carried out to justify the efficiency of doubler plate in strengthening CHS T-joints against cyclic loads. An experimental study was performed on four full-scale specimens, two with doubler plate, and the others without the reinforced plate. The joint capacity of hysteretic curve plotting was extracted from the experimental results. A finite element analysis study was conducted using the ABAQUS software package and results were in favorable agreement with the experimental findings. The effect of chord stiffness α on the joint capacity required the extension of a numerical study with an additional Finite Element Model (FEM). The current research justified the improvement of joint positive capacity by 40%, and enhancement of negative capacities by 70%. The relation between capacity and α is expressed by an empirical equation Enhancement in energy dissipation was confirmed with the existence of doubler reinforced plate.

Keywords: Cyclic load, Hysteresis, T joint, Doubler Plate, Joint Capacity, Dissipated Energy, Stress Distribution

1. INTRODUCTION

Circular Hollow Sections CHS are used extensively in steel structure due to their flexural and torsional rigidity. This manuscript studies the behavior of CHS T-joints subjected to cyclic load. The study concentrates on two types of CHS T-joints (unreinforced and reinforced with doubler). The research lays out previous experimental and numerical studies basic to well understand the behavior of joints subjected to cyclic load. In his work [1], has numerically performed on CHS X-joints reinforced with doubler plate exposed to in plane bending taken the effect of variation of geometric parameters. Joint capacity was enhanced by 240% for reinforced joints relative to un-reinforced joint. Based on which, an empirical equation was extracted to express strength of joints reinforced with doubler plate. Numerically the study investigated the influence of adding doubler plate to tubular T/Y-joints on the ultimate strength, initial stiffness, and failure mechanisms. Through FEM, a series of models were simulated to determine the impact of the doubler plate's geometry in enhancing the static strength of the T/Y-joints. In comparison with the unreinforced joint, the T/Y joints reinforced with doubler plate were found to have considerably increased their initial stiffness, and improved their failure mode by up to 295% [2].

Experimental and numerical investigations on collar and doubler plates reinforced with square hollow section SHS T-joints under axial compression. Specimens in different brace to chord width ratio (β)–were tested. Joint capacity was enhanced significantly with reinforced joints. The increase of the doubler plate thickness has improved the strength and ductility of the reinforced SHS T-joints under axial compression. Corresponding Finite Element Model (FEM) was performed with results matching those of the experiments [3]. The effect of cyclic load on material behavior should be considered, isotropic and kinematic hardening parameters should be determined[4]. These hardening parameters were obtainable from tensile coupon test [5], and provided an acceptable material representation when subjected to cyclic load. As presented above, hollow section joints studied with static load (as axial or bending). This manuscript verified the improvement occurred on CHS T-joints reinforced with doubler plate subjected to cyclic load. Experimental study was performed on four specimens, two with doubler and the others without reinforced plate. Cyclic load was applied through load protocol in compliance with FEMA-461 [6], hysteresis curve extracted from the experimental work was the basis to understand joint behavior. Numerical study was compared with the experiment results, and findings were in positive agreement. The numerical study was extended with additional FEM to thoroughly understand the behavior and measure improvement in the reinforced joints.

2. TEST PROCEDURE

Experimental work was conducted to study the behavior of CHS T-joint reinforced with Doubler plate and unreinforced (Default) subjected to cyclic load. The behavior was checked and compared through failure observation, hysteresis curve and joint capacity.

TABLE 1 *Experiment Specimens*

Specimen No.	T-joint Type	Chord		Brace		Doubler	
		D (mm)	T (mm)	d (mm)	T (mm)	Dd (mm)	Td (mm)
SP01	Default	114	3	114	3		
SP02	Default	88	3	114	3		
SP03	Doubler	114	3	114	3	126	6
SP04	Doubler	88	3	114	3	126	6

- *Hanan H. Eltobgy, Associate Professor, Civil Eng. Department, Faculty of Engineering, Shoubra, Benha University, Egypt. E-mail: hanan.eltobgy@feng.bu.edu.eg*
- *Emad Darwish, Lecturer, Civil Eng. Department, Faculty of Engineering, Shoubra, Benha University, Egypt. E-mail: emad.darwish@feng.bu.edu.eg*
- *Mohamed A. Aboshok, Assistant Lecturer, Civil Eng. Department, Faculty of Engineering, Shoubra, Benha University, Egypt. E-mail: mohamed.aboshok@feng.bu.edu.eg*

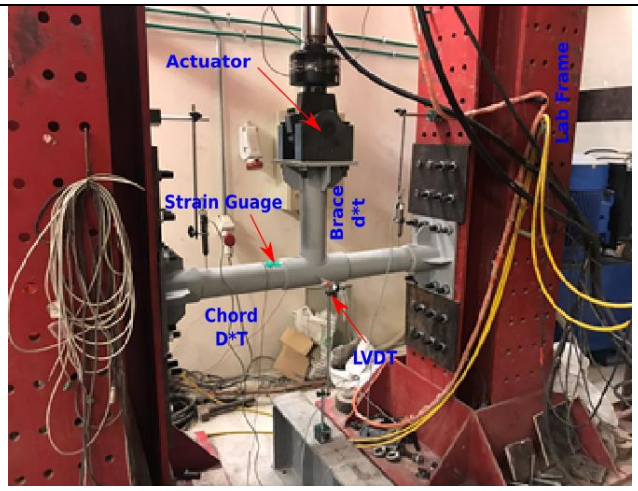

***Fig. 1**. Experiment Setup*

. In the material mechanical properties identified through coupon test, the yield and ultimate strength were 326 and 460 Mpa, respectively. Specimens were fabricated and erected on laboratory frame as shown in Fig. 1. Cyclic load was applied through a single ended servo-controlled actuator operated by load protocol based on the Federal Emergency Management Agency, FEMA-461 [6]. Load

2.1. Specimens and Setup

Four specimens were selected to compare the behavior between the concerned types, two represented the unreinforced joints (SP01 and SP02), and the others exemplified the joints reinforced joint with doubler (SP03 & SP04). Joint geometry parameters are listed in

protocol was governed by joint yield displacement calculated from a monotonic test. Load displacement data has been extracted through a digital data acquisition system Model DTE~500 connected to a personal computer.

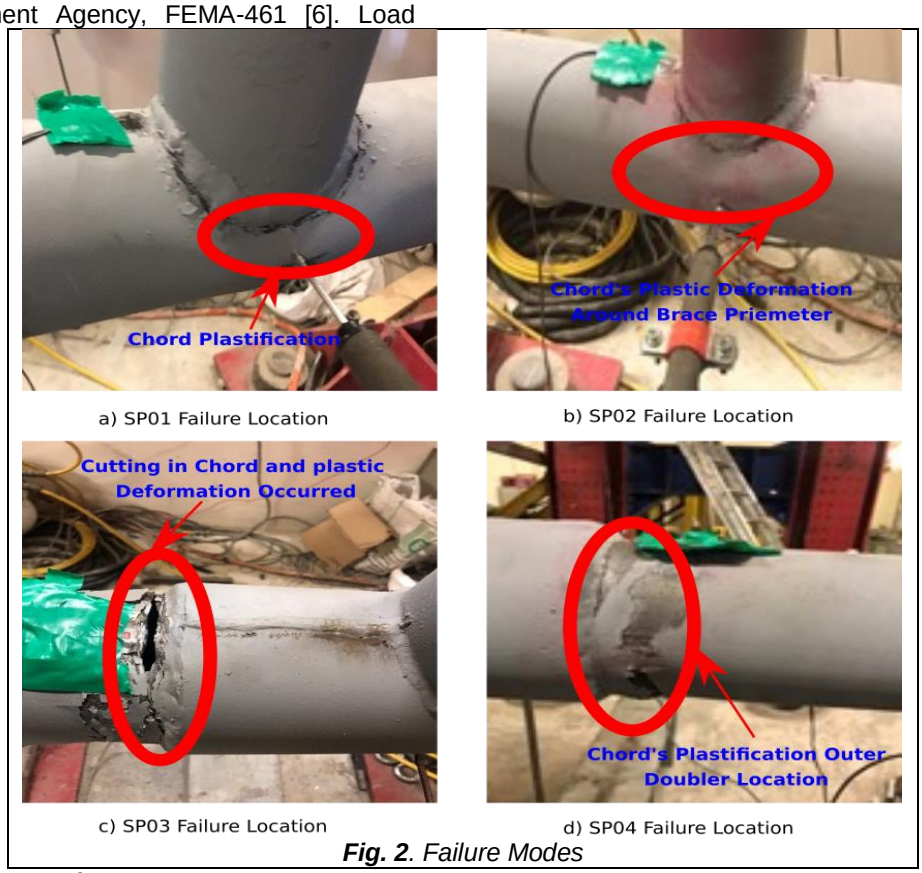

***Fig. 2**. Failure Modes*

2.2. Failure Mode Observations

Failure mechanism has been different between tested specimens. For SP01 and SP02, test was terminated after 15 cycles and plasticity of chord around connection location would govern the failure mode. Specimens with doubler could sustain till 17 cycles and the failure mode was chord's plasticity outbound the doubler length and cutting in chord was occurred as shown in Fig. 2. Initial stiffness of chord at connection location was increased, therefore, reinforced specimens can sustain more cycles and distribute stress around connection perimeter.

2.3. Hysteresis Curve

Hysteresis curve plotted from load displacement data was extracted from laboratory instruments. Curve should be analyzed to obtain S curve resulting from the identification of the inflection points on curve, and the connection between them as shown in Fig. 3 to **Error! Reference source not found.**. Positive and Negative capacities (P_{u+ve} and P_{u-ve}) and displacement (Δ_y and Δ_u) could be obtained from S curve as listed in TABLE ***2***
.

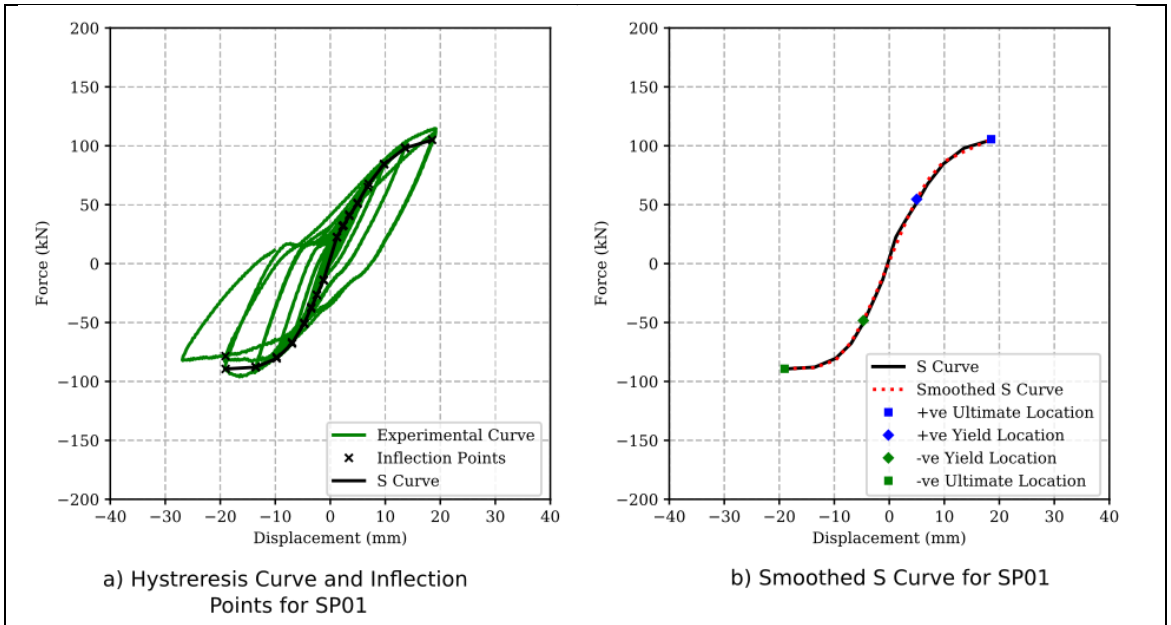

a) Hystreresis Curve and Inflection Points for SP01

b) Smoothed S Curve for SP01

Fig. 3*. Hysteresis Curve and S Curve for SP01*

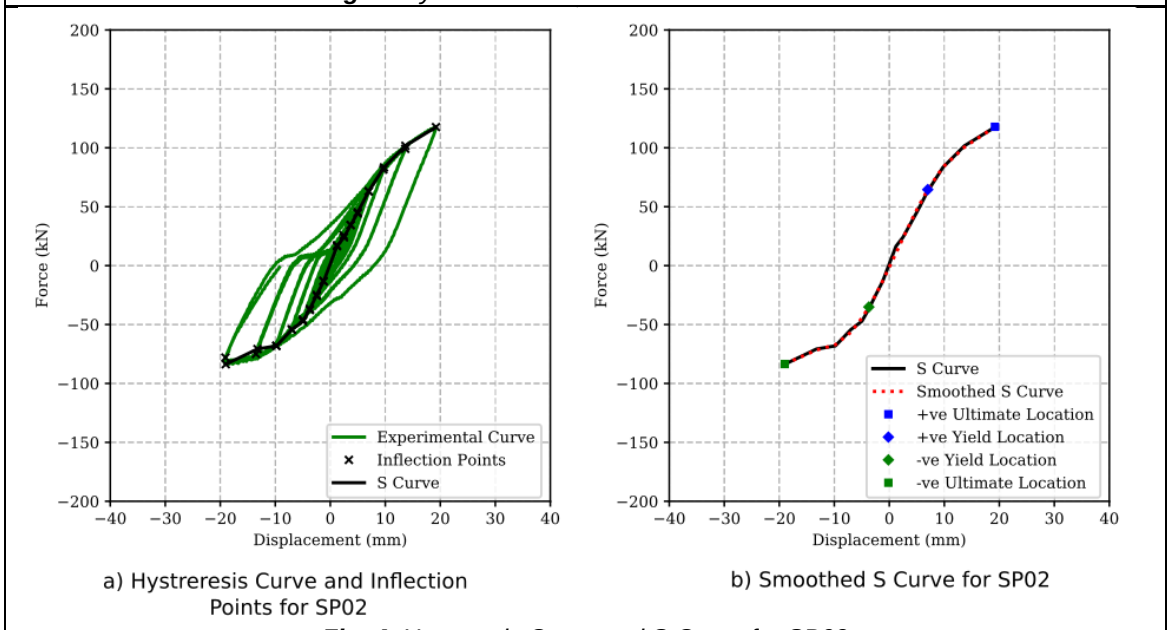

a) Hystreresis Curve and Inflection Points for SP02

b) Smoothed S Curve for SP02

Fig. 4*. Hysteresis Curve and S Curve for SP02*

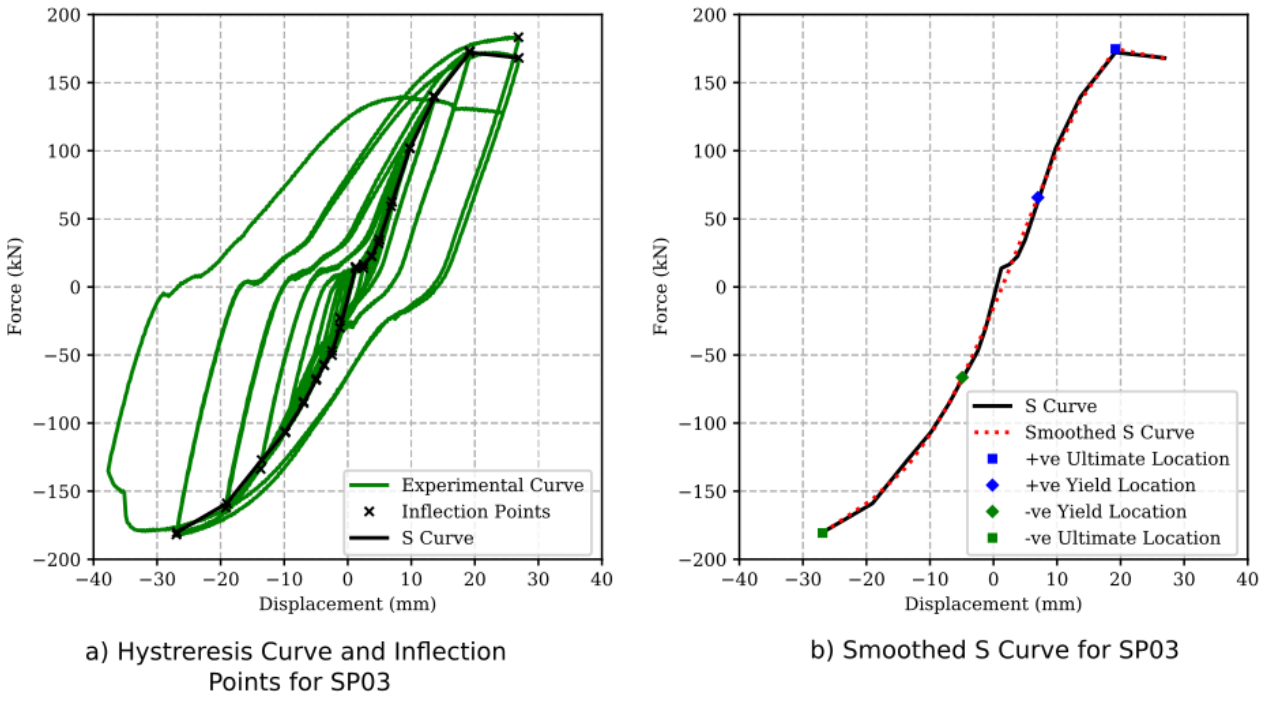

***Fig. 5**. Hysteresis Curve and S Curve for SP03*

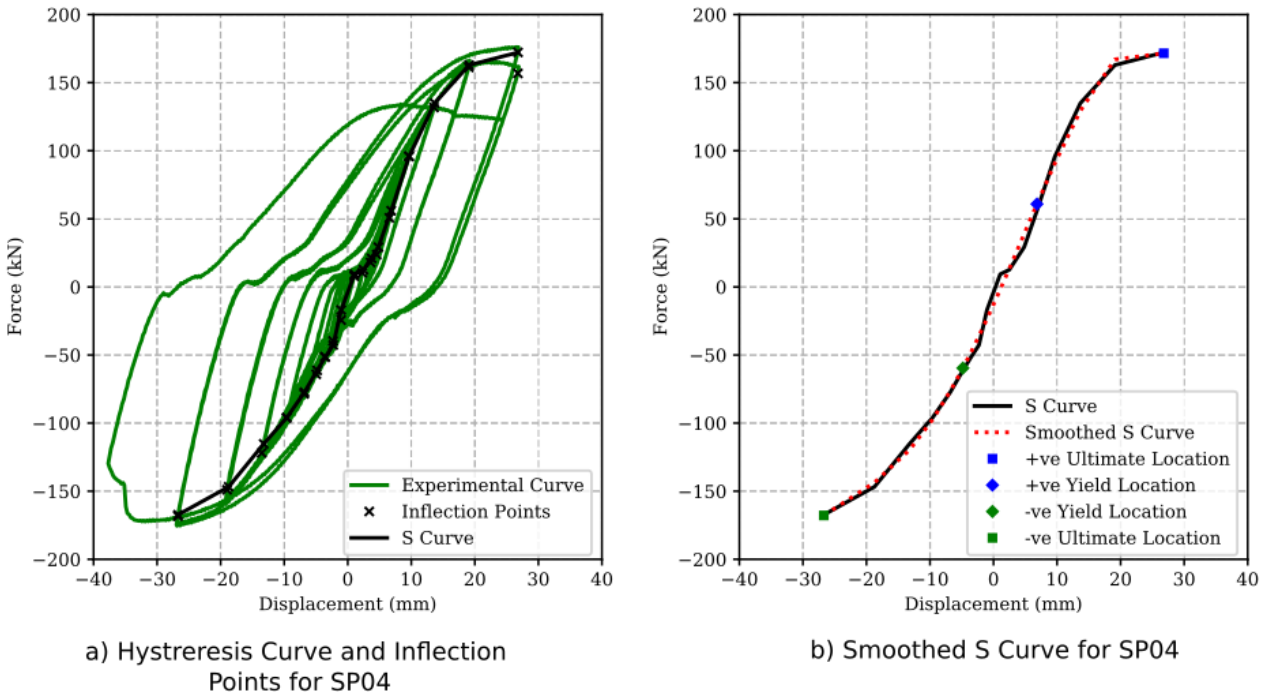

***Fig. 6**. Hysteresis Curve and S Curve for SP04*

TABLE 2

Positive and Negative Capacities Extracted from S Curve

Specimen No.	Displacement				Force			
	Δ_{y+ve} (mm)	Δ_{u+ve} (mm)	Δ_{y-ve} (mm)	Δ_{u-ve} (mm)	P_{y+ve} (KN)	P_{u+ve} (KN)	P_{y-ve} (KN)	P_{u-ve} (KN)
SP01	4.98	18.52	-4.71	-19.03	54.62	105.58	-48.33	-89.23
SP02	6.99	19.21	-3.72	-19.00	64.54	117.80	-35.10	-83.53
SP03	6.98	19.18	-4.92	-26.90	65.64	174.67	-66.45	-180.66

SP04	6.84	26.79	-4.82	-26.71	60.87	171.57	-59.61	-167.79

3. FINITE ELEMENT MODEL (FEM)

FEM was conducted by the applications of ABAQUS software and verified by the experimental results. Weld simulation and residual stress were ignored in FEM [7]. Comparison between the experimental and numerical investigations has been conducted through hysteresis curve, joint capacity, and energy dissipation.

3.1. FEM Inputs

FEM has been performed through defining model input data (parts, material, boundary condition, mesh, step, and history output). 3D Solid Deformable part was defined for connection components. Material parameters defined as density, elastic and plastic ranges were extracted from the coupon test. Combined hardening parameters were assigned for material behavior under cyclic load. A kinematic and isotropic hardening material models were adopted with properties taken from the tensile coupon tests [8]. Damage and fracture mechanisms were not applied into the FE model. General static analysis was applied on FEM with a step for each amplitude in the load cycle. Boundary condition at the ends was simulated with end plates to represent the experimental setup, where the end plates were restrained at bolt locations. Load was applied in model as displacement control at reference point with amplitude value in load protocol. Finer mesh was created at the intersection zone of connection to obtain a representative stress distribution value as shown in Fig. 7. Tetrahedral elements (C3D8R) are geometrically versatile therefore, used in many automatic meshing algorithms. Resultant parameters were determined through History and field outputs.

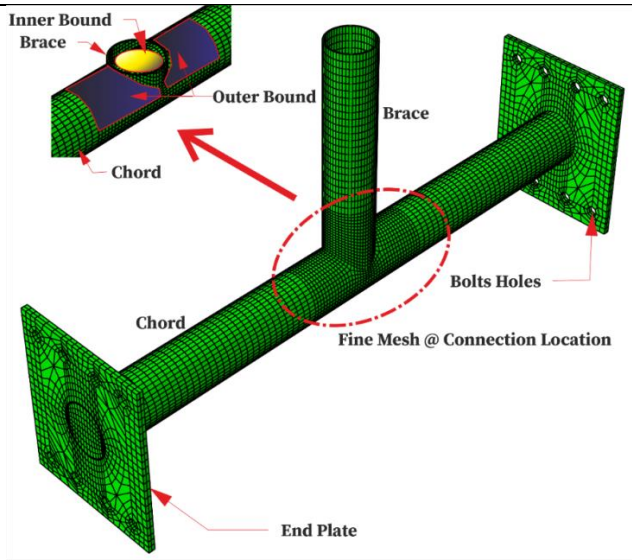

***Fig. 7**. Inner and Outer Bound at connection Location*

3.2. Hysteresis Curve

Load displacement curves for specimens were plotted from history output variables. Manual termination has been defined in FEM results since, the analysis did not obtain a fracture mechanism. Comparison was conducted between hysteresis curves, FEM in magnetic color, and experiment curve in green. It was noticed that, the behavior of hysteresis curves was almost similar in all tested specimens as shown in Fig. 8. S curves extracted from hysteresis curve and yield, as well as the ultimate domains for positive and negative zones could be obtained as shown in **Error! Reference source not found.**. For positive zone, yield domain (Δ_{y+ve} and P_{y+ve}) is in diamond blue symbol and ultimate domain (Δ_{u+ve} and P_{u+ve}) is plotted in square blue symbol. Negative yield domain (Δ_{y-ve} and P_{y-ve}) is determined with diamond green symbol, and negative ultimate domain (Δ_{u-ve} and P_{u-ve}) presented in square green. Capacities of FEM results were in positive agreement with experimental results as listed in

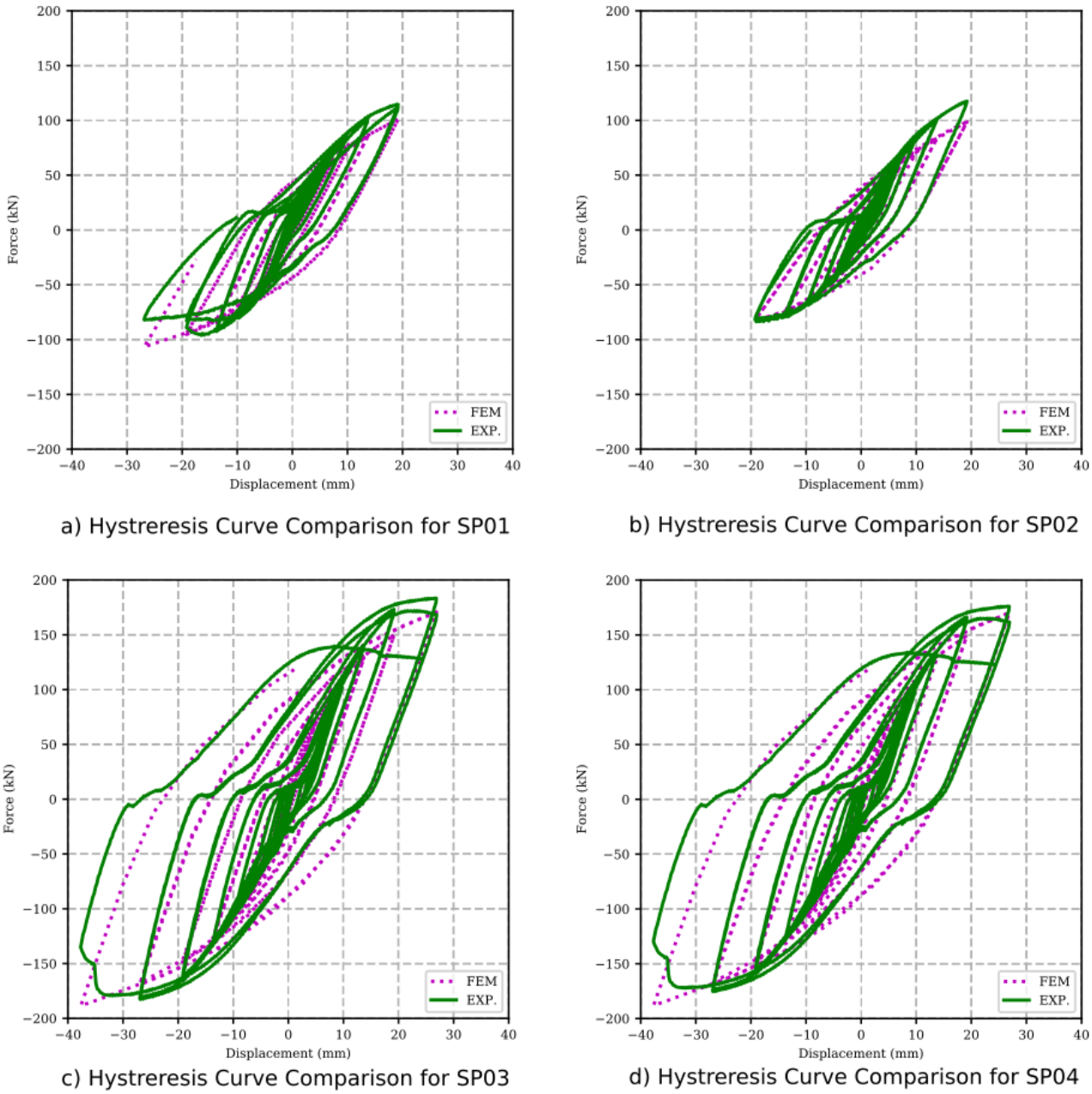

***Fig. 8**. Hysteresis Curve Comparison between FEM and EXP.*

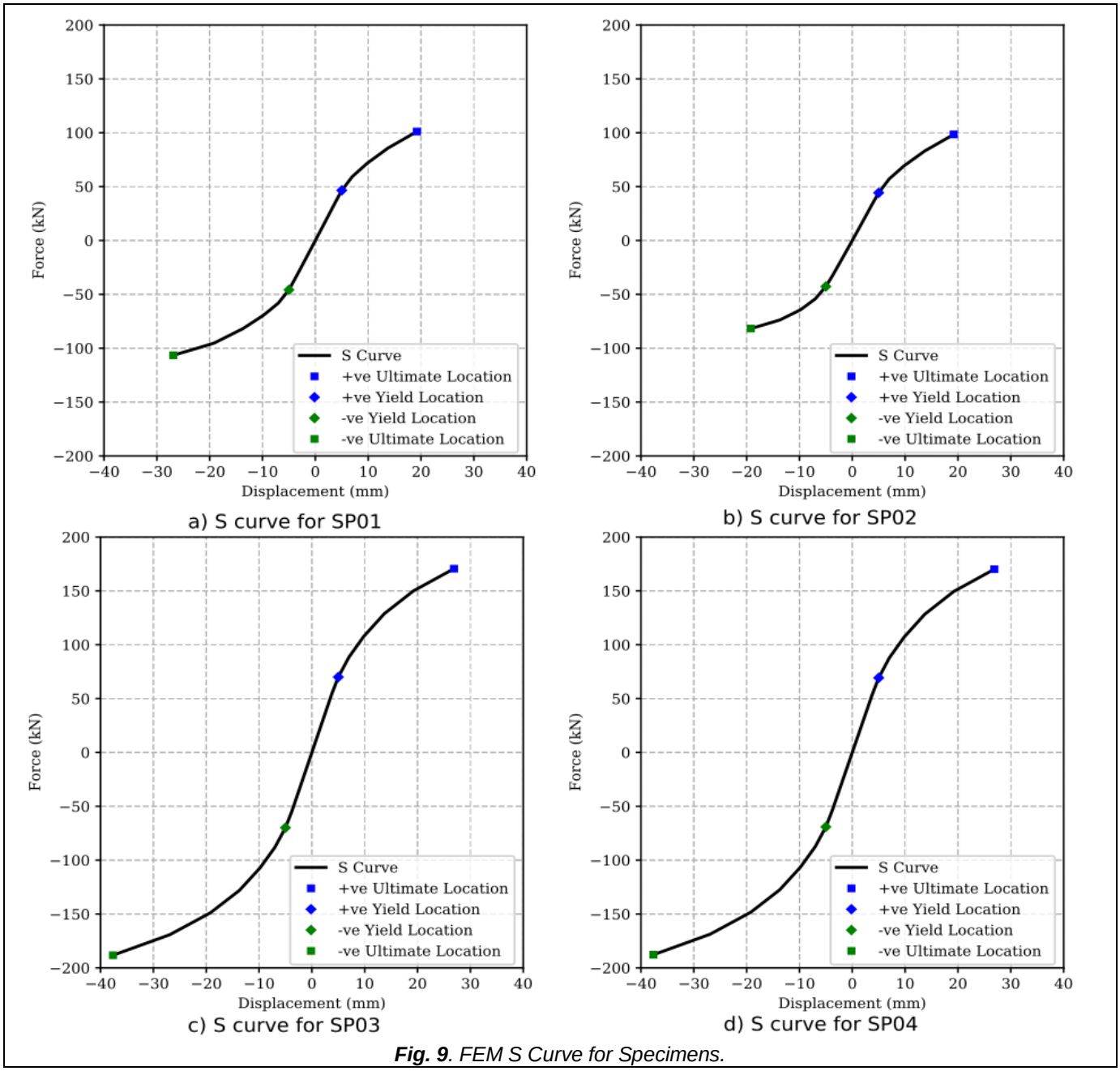

***Fig. 9**. FEM S Curve for Specimens.*

TABLE 3
Ultimate Capacity of CHS T-Joints, Experimental and FEM

Specimen No.	Experiment		FEM		% diff of P_{u+ve}	% diff of P_{u-ve}
	P_{u+ve}	P_{u-ve}	P_{u+ve}	P_{u-ve}		
SP01	105.58	-89.23	101.13	-106.57	-4.21%	19.43%
SP02	117.80	-83.53	98.72	-81.79	-16.20%	-2.08%
SP03	174.67	-180.66	170.57	-188.23	-2.34%	4.19%
SP04	171.57	-167.79	170.12	-187.78	-0.84%	11.91%

3.3. Energy Dissipation

Joint dissipation energy was an index to measure the behavior of different types of CHS T-joints. It can be calculated through cumulative area engulfed by each loading cycle in hysteresis curve. Overall energy for specimens were 18.81, 16.79, 42.29 and 40.84, KN.m, corresponding to SP01 to SP04, respectively as shown in Fig. 10.

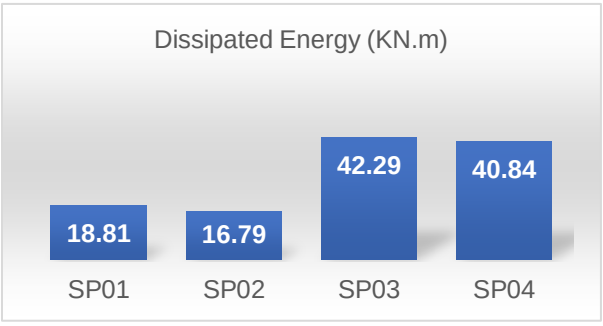

***Fig. 10**. Dissipated Energy for Specimens*

3.4. Stress Distribution

Distribution of stress and plastic strain leads were applied to predict locations of cracks around brace in connection. Default Type displayed a stress concentration around brace location (inbound and outbound zones) loaded into plastic deformation at crown location as shown in Fig. ***11***a& b. For other specimens with doubler reinforced, the plate has increased the load capacity and ductility of joint by redistribution of stress over a large area. For joint with doubler described in Fig. 11c& d, stress concentration reached the same limits of doubler, therefore, the location of plastic strain and cracks has been transferred away from the brace location.

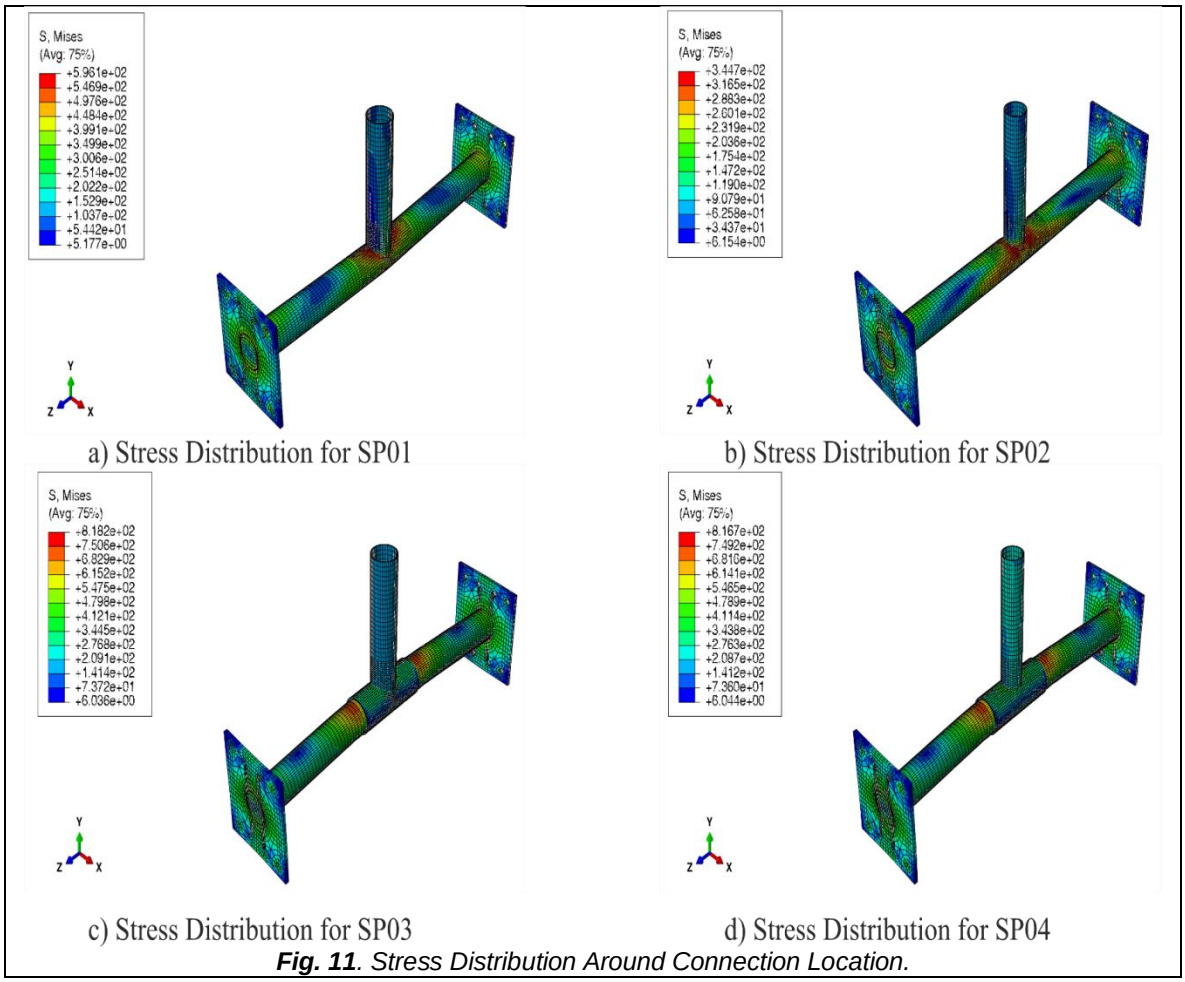

***Fig. 11**. Stress Distribution Around Connection Location.*

4. PARAMETRIC STUDY

Numerical study was extended with a larger number of FEM to better understand the behavior of joints under cyclic load. This research studied the joint capacity with change in brace to chord diameter (α=d/D) where d represents the brace diameter, and D the chord diameter as shown in Fig. 12. Number of models in parametric study were selected to cover geometrical validity as per CIDECT design guide [9] and Chinese Code [10]. Range validity for α was between 8.00 and 40.00. The corresponding models and profiles are listed in

TABLE 4 for two types T01 (default type) and T02 (doubler type). Load and displacement versus time data would be extracted from the history output of FEM, and the related data could be analyzed to get the hysteresis curve. Stress distribution and determination of stress concentration location were plotted from the field output of FEM. Analysis of data and comparison among different types are illustrated in the following sections.

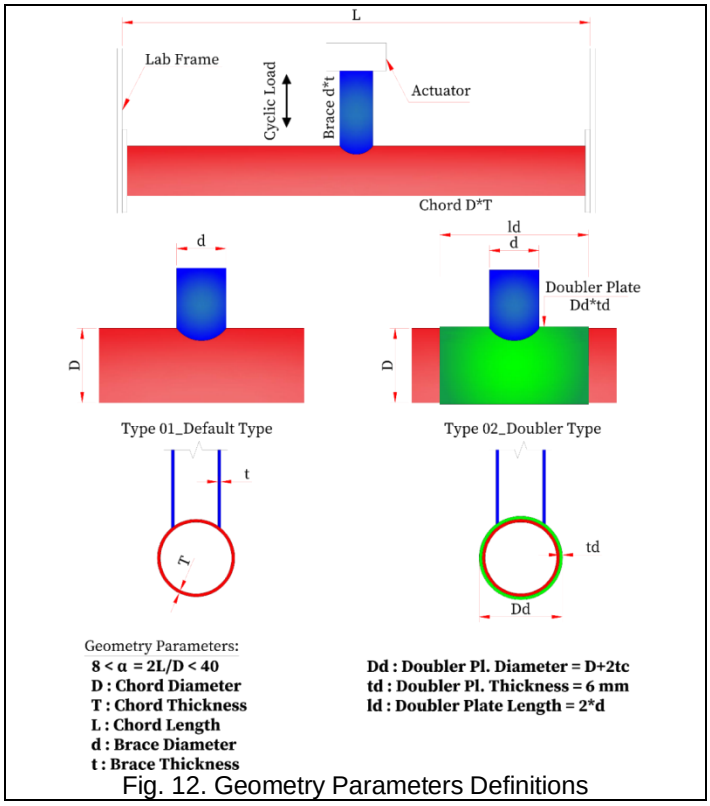

Fig. 12. Geometry Parameters Definitions

TABLE 4
Parametric Study Models

Default Joints	Doubler Joints	Brace		Chord		Length L (mm)	α
		d (mm)	t (mm)	D (mm)	T (mm)		
T01-01	T02-01	323.9	8	323.9	8	2000	12.35
T01-02	T02-02	177.8	6	355.6	6.3	2500	14.06
T01-03	T02-03	323.9	6	323.9	8	2500	15.44
T01-04	T02-04	88.9	6	177.8	10	1500	16.87
T01-05	T02-05	101.6	4	168.3	10	1500	17.83
T01-06	T02-06	193.7	6	193.7	6	2000	20.65
T01-07	T02-07	139.7	3.2	139.7	8	1500	21.47
T01-08	T02-08	193.7	6	193.7	6	2500	25.81

4.1. Joint Capacity

Behavior of joints have been studied through output comparison variable as positive and negative joint capacities. Variables were evaluated from the hysteresis curve plotted from the load displacement data of FEM, extracting S curves for each model.

Joints capacities were extracted from S curve and filtered to Fig. out the effect of each parameter on positive and TABLE 5 for all types.

The existence of doubler has improved joint capacity at the smaller values of α, when α = 12.35, and increased positive capacity by 40%, however, this improvement decreased gradually at α =17.84. No remarkable improvement was noticed in positive capacity when α >18. Enhancement in negative capacity was achieved by 70 % when α =12.35 and gradually decreased to 20 % at α=17.84 as shown in Fig. 13.

We can conclude from the behavior above that, when α value was small, the stiffness of chord increased and the failure mode at connection governed the connection capacity, accordingly, doubler plates increased the capacity at the smaller value of α.

negative capacities (P_{u+ve} and P_{u-ve}). The data are plotted as scatter diagram with dotted red color for P_{u+ve} and x red color for P_{u-ve}, then smoothed to curve in blue for positive capacity and green for negative capacity. Relation between change in α and joint capacity is described below. Joint capacity extracted from S curve for the filtered models are listed in

TABLE 5
Positive and Negative Capacities for T01 & T02

α	Positive Capacity (KN)		Negative Capacity (KN)	
	T01	T02	T01	T02
12.35	1221.50	1709.30	-887.43	-1507.30
14.06	784.34	1036.80	-236.93	-537.20
15.44	968.96	1270.40	-772.88	-1192.70
16.87	548.95	685.76	-365.29	-644.47
17.83	525.45	524.33	-401.35	-526.51
20.65	370.36	462.61	-323.23	-455.54
21.47	321.69	418.26	-301.39	-412.23
25.81	297.75	355.93	-255.81	-351.75

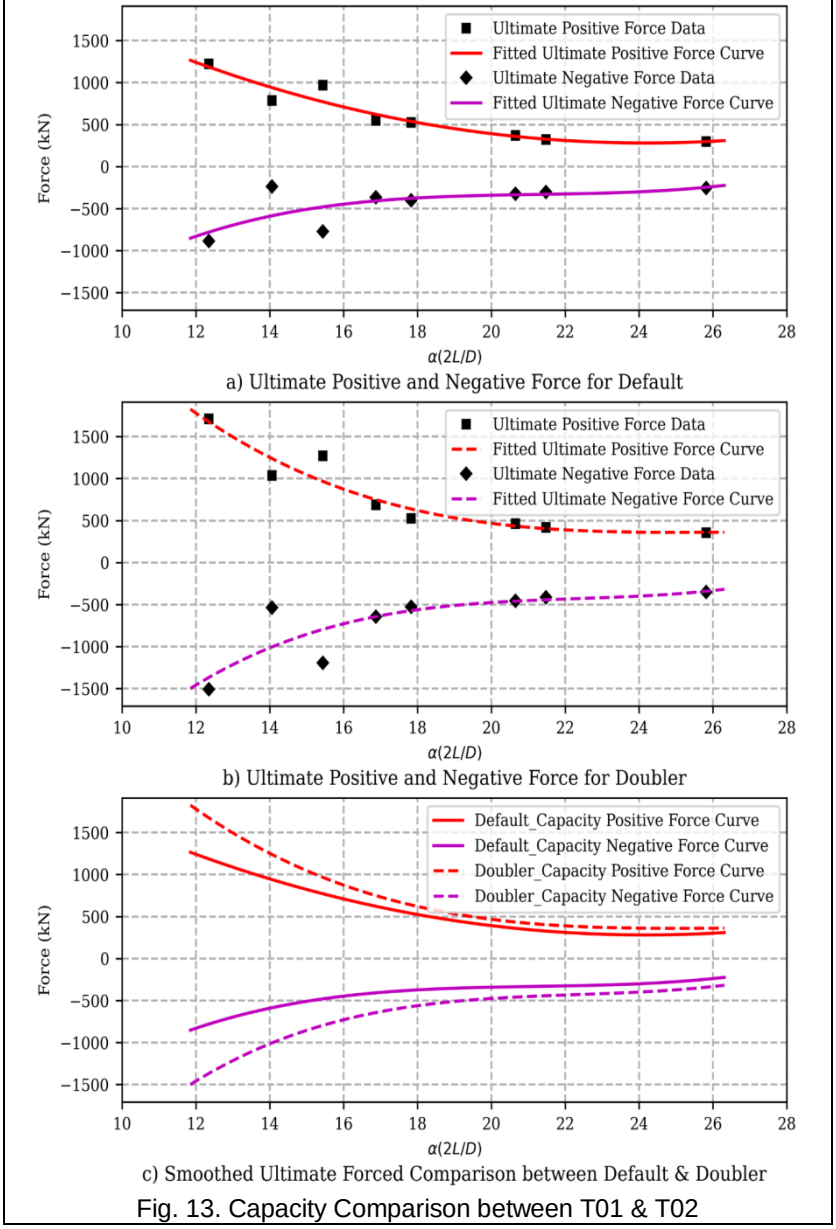

Fig. 13. Capacity Comparison between T01 & T02

For T01, positive capacity can be expressed by the fitting equation described in (1) and improved positive capacity using doubler is presented in (2).

$$P_{u+ve\_T01} = (0.02\alpha^2 - 1.01\alpha + 12.82)F_y \quad \text{(KN)} \quad (1)$$

$$P_{u+ve\_T02} = (0.12\alpha^2 - 3.21\alpha + 29.00)F_y \quad \text{(KN)} \quad (2)$$

Negative capacity can be formatted with the following equations (3) and (4) for T01 and T02, respectively.

$$P_{u-ve\_T01} = (-0.11\alpha^2 + 2.30\alpha - 17.60)F_y \quad \text{(KN)} \quad (3)$$

$$P_{u-ve\_T02} = (-0.16\alpha^2 + 3.65\alpha - 29.20)F_y \quad \text{(KN)} \quad (4)$$

4.2. Dissipated Energy

More chord's stiffness more ability to dissipate energy, comparison among joints was performed to measure the improvement occurred after using reinforcing tools as shown in TABLE 6.

Improvement remarked by 70 % in energy dissipation at α=12 and decreased as α increased. Unremarkable enhancement is observed when α was 20.0 as shown in

Fig. 14. Dissipated Energy for T01 & T02

.

TABLE 6
Dissipated Energy for Parametric Study

α	Dissipation Energy (KN. m)	
	T01	T02
12.35	631.16	1052.60
14.06	309.08	538.07
15.44	665.77	1025.96
16.87	231.22	326.02
17.83	204.73	135.14
20.65	228.85	286.47
21.47	159.42	225.55
25.81	270.91	332.84

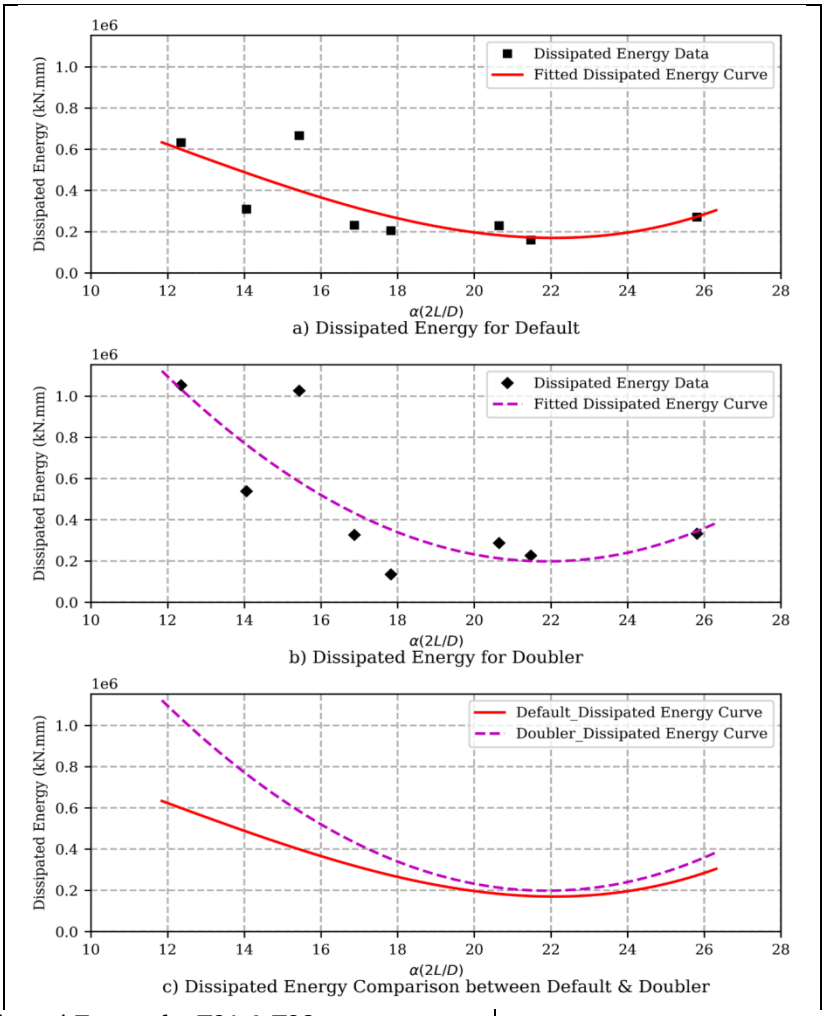

Fig. 14. Dissipated Energy for T01 & T02

4.3. Stress Distribution

Stress distribution can be a sign to predict the locations of stress concentration as well as locations of cracks propagation.

In chord with large stiffness (small α) the stresses are concentrated around perimeter of brace, inbound and outbound zones subjected to medium and low stress. Otherwise, stress would be high at zones around brace location when α is larger than 20 as shown in Fig. 15.

Doubler plate confined chord around connection and increased initial stiffness at connection location. Stress concentration transfers outbound of doubler length as shown in Fig. 16.

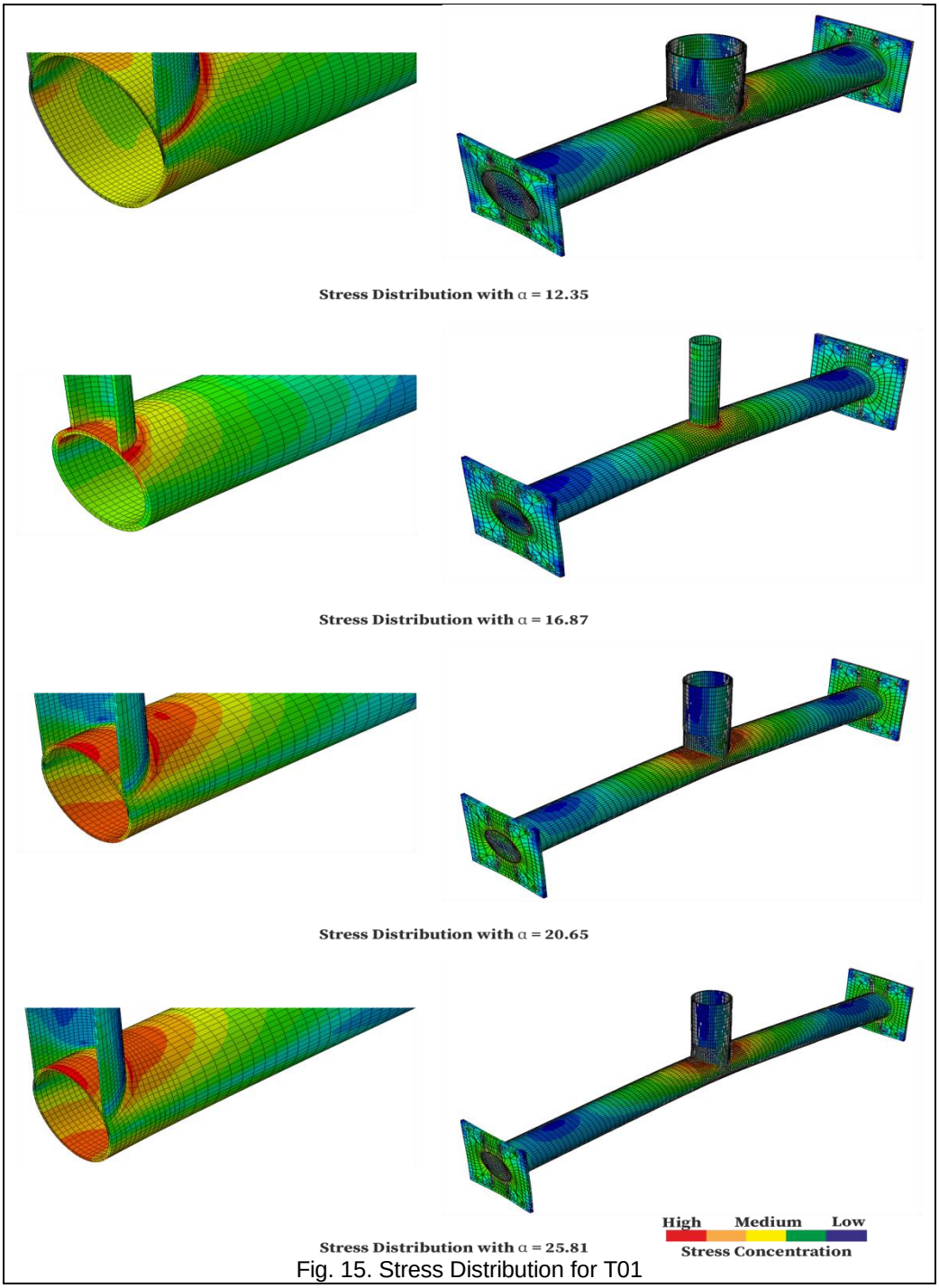

Fig. 15. Stress Distribution for T01

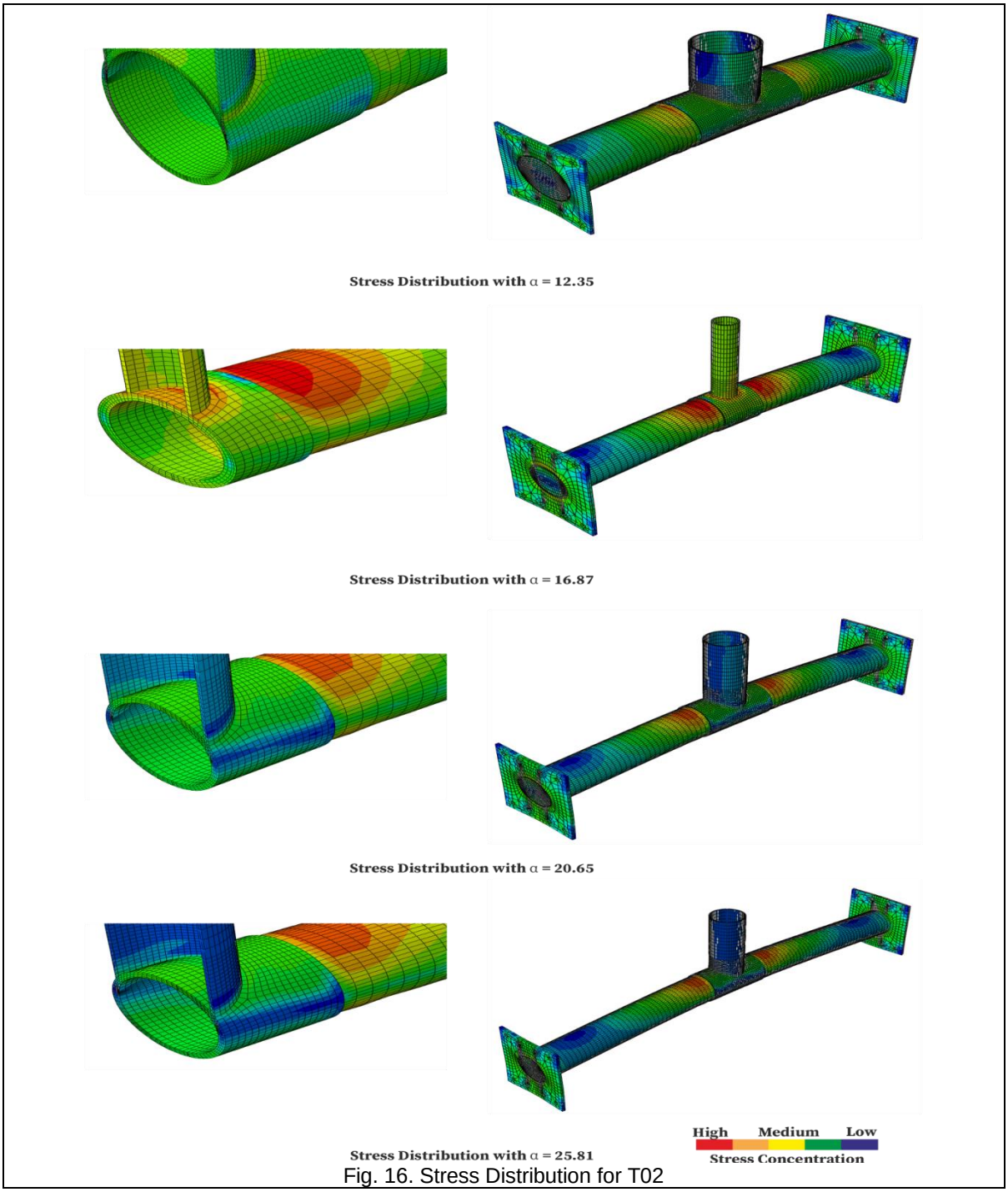

Fig. 16. Stress Distribution for T02

5. SUMMARY AND CONCLUSIONS

Contemporary years have witnessed significant advances in the investigation of CHS T-joints' behavior. Research in these domains is usually carried out using various types of static load (axial tension, axial compression and bending). This study meant to investigate the improvement in CHS T joint through reinforcement with doubler plate subjected to cyclic load. Experimental study was performed on two different types of specimens, two were the default type connection, and the others were reinforced chord with doubler. Hysteresis curve was plotted from load displacement data. FEM was performed using ABAQUS software applications and verified by experimental results. Hysteresis curve was obtained from FEM results extracting the joint capacities. The results from FEM were in positive agreement with the experimental study.

The outcome of experimental and numerical study leads to the conclusion that doubler pipe increased the joint load capacity by 50% than the default type in tension cycles, and by 100% in compression cycles. Doubler increased the initial stiffness of chord at connection location, accordingly, enhancement in joint behavior has occurred under cyclic load.

Parametric study was conducted with change in geometry parameter β that represent chord's stiffness. Positive capacity with doubler has gradually been increased from 40% corresponding to α = 12.35, whereas, negative. capacity increased by 70 % at α =12.35 and gradually decreased to 20 % at α=17.84. Improvement in energy

dissipation was remarked by 70 % at α=12.35. This means that more chord's stiffness reflected on more ability to dissipate energy. Doubler plate confined chord around connection consequently increased the initial stiffness at connection location, and stress concentration transfer of the outbound of doubler length.

6. REFERENCES

[1] Y. S. Choo, J. X. Liang, G. J. der Vegte, and J. Y. R. Liew, “Static strength of collar plate reinforced CHS X-joints loaded by in-plane bending,” J. Constr. Steel Res., vol. 60, no. 12, pp. 1745–1760, 2004.

[2] H. Nassiraei, M. A. Lotfollahi-Yaghin, and H. Ahmadi, “Static strength of doubler plate reinforced tubular T/Y-joints subjected to brace compressive loading: Study of geometrical effects and parametric formulation,” Thin-Walled Struct., vol. 107, pp. 231–247, 2016.

[3] R. Feng, Y. Chen, and D. Chen, “Experimental and numerical investigations on collar plate and doubler plate reinforced SHS T-joints under axial compression,” Thin-Walled Struct., vol. 110, no. October 2016, pp. 75–87, 2017.

[4] V. Abaqus, “6.14 Documentation,” Dassault Syst. Simulia Corp., vol. 651, pp. 2–6, 2014.

[5] C. I. Zub, A. Stratan, and D. Dubina, “Calibration of parameters of combined hardening model using tensile tests,” 2020.

[6] F. FEMA, “461-Interim protocols for determining seismic performance characteristics of structural and nonstructural components through laboratory testing, Federal Emergency Management Agency (FEMA), Document No,” Redw. City, CA, 2007.

[7] Y.-B. Shao, T. Li, T. L. Seng, and S.-P. Chiew, “Hysteretic behaviour of square tubular T-joints with chord reinforcement under axial cyclic loading,” J. Constr. Steel Res., vol. 67, no. 1, pp. 140–149, 2011.

[8] C. I. Zub, A. Stratan, and D. Dubina, “Calibration of parameters of combined hardening model using tensile tests,” SDSS 2019 - Int. Colloq. Stab. Ductility Steel Struct., 2019.

[9] J. Wardenier and J. Wardenier, Design guide for circular hollow section (CHS) joints under predominantly static loading. Cidect, 2008.

[10] C. S. GB50017, “Code for design of steel structures,” Ministry of construction of the People’s Republic of China. China Planning Press Beijing, 2003.